# Clauser-Horne inequality for electron-counting statistics in multiterminal mesoscopic conductors

Lara Faoro,[1,2] Fabio Taddei,[1,3] and Rosario Fazio[3]
[1] *ISI Foundation, Viale Settimio Severo, 65, I-10133 Torino, Italy*
[2] *Department of Physics and Astronomy, Rutgers University, 136 Frelinghuysen Road, Piscataway, New Jersey 08854, USA*
[3] *NEST-INFM & Scuola Normale Superiore, I-56126 Pisa, Italy*

(Received 1 July 2003; revised manuscript received 5 November 2003; published 18 March 2004)

In this paper we derive the Clauser-Horne (CH) inequality for the full electron-counting statistics in a mesoscopic multiterminal conductor and discuss its properties. We first consider the idealized situation in which a flux of entangled electrons is generated by an *entangler*. Given a certain average number of incoming entangled electrons, the CH inequality can be evaluated for different numbers of transmitted particles. Strong violations occur when the number of transmitted charges on the two terminals is the same ($Q_1 = Q_2$), whereas no violation is found for $Q_1 \neq Q_2$. We then consider two actual setups that can be realized experimentally. The first one consists of a three terminal normal beam splitter and the second one of a hybrid superconducting structure. Interestingly, we find that the CH inequality is violated for the three terminal normal device. The maximum violation scales as $1/M$ and $1/M^2$ for the entangler and normal beam splitter, respectively, $2M$ being the average number of injected electrons. As expected, we find full violation of the CH inequality in the case of the superconducting system.

DOI: 10.1103/PhysRevB.69.125326 PACS number(s): 73.23.−b, 72.70.+m, 03.65.Ud, 74.40.+k

## I. INTRODUCTION

Entanglement[1] denotes the nonlocal correlations that exist, even in the absence of direct interaction, between two (spatially separated) parts of a given quantum system. Entanglement is believed to be the main ingredient of computational speed-up in quantum information protocols. Because of its fundamental importance, a great deal of interest has been brought forth by its role in quantum information.[2]

Most of the work on entanglement has been performed in optical systems with photons,[3] cavity QED systems,[4] and ion traps.[5] Only recently attention has been devoted to the manipulation of entangled states in a solid-state environment. This interest, originally motivated by the idea to realize a solid-state quantum computer,[6–8] has been rapidly growing and by now several works discuss how to generate, manipulate, and detect entangled states in solid-state systems. It is probably worth to emphasize already at this point that, differently from the situation encountered in quantum optics, in solid-state systems entanglement is rather common. What is not trivial is its control and detection (especially if the interaction between the different subsystems forming the entangled state is switched off).

Despite the large body of knowledge developed in the study of optical systems, new strategies have to be designed to reveal the signatures of nonlocal correlations in the case of electronic states. For mesoscopic conductors, the prototype scheme was discussed in Ref. 9. In this work it has been shown that the presence of spatially separated pairs of entangled electrons, created by some *entangler*, can be revealed by using a beam splitter and by measuring the correlations of the current fluctuations in the leads. Provided that the electrons injected are in an entangled state, bunching and antibunching behaviors for the cross-correlations of current fluctuations are found depending on whether the state is a spin singlet or a spin triplet. Not only the noise, but the full counting statistics is sensitive to the presence of entanglement in the incoming beam.[10] The distribution of transmitted electrons is binomial and symmetric with respect to the average number of transmitted charges. Moreover, this is important for the problem studied in the present work, the joint probability for counting electrons at different leads unambiguously characterizes the state of the incident electrons if one uses spin-sensitive electron counters. In this case the joint probability cannot be expressed as a product of single-terminal probabilities.

Given the general setup to detect entanglement, an important issue is to understand how to generate it. This has been discussed in several papers. Most of the existing proposals are based on the generation of Bell states by means of electron-electron interaction. This can be achieved through superconducting correlations[11] in hybrid normal-superconducting[12–15] and superconductor–carbon nanotubes systems,[16–18] quantum dots in the Coulomb blockade regime,[19] or Kondo-like impurities.[20] Then, by using energy or spin filters, the two electrons forming the Bell state are separated. The entanglement can be created in the spin or in the orbital[15] degrees of freedom. Very recently, as is also discussed in Sec. III C, it was shown that in a mesoscopic multiterminal conductor entanglement can be produced also in the absence of electron interaction.[21] Besides electrons, it is possible to produce entangled states with Cooper pairs in superconducting nanocircuits[22] or by coupling a mesoscopic Josephson junctions with superconducting resonators.[23–26]

Since Bell's work,[27] it is known that a classical theory formulated in terms of a hidden variable satisfying reasonable condition of locality, yields predictions which are different from those of quantum mechanics. These predictions were casted into the form of inequalities which any realistic local theory must obey. Bell inequalities have been formulated for mesoscopic multiterminal conductors in Refs. 15, 21, and 28–31 in terms of electrical noise correlations at different terminals.[32] A test of quantum mechanics through Bell inequalities in mesoscopic physics is very challenging and most probably it would be rather difficult, if not impossible, to get around all possible loopholes. Although solid-state systems are not the natural arena where to test the foundations of quantum mechanics, it is nevertheless very interesting to access, manipulate, and quantify these nonlocal correlations.

In this work we derive a Bell inequality for the full electron-counting statistics and discuss its properties. The formulation we follow is based on what is known as the Clauser-Horne (CH) inequality.[33,34] We shall show that the joint probabilities for a given number of electrons to pass through a mesoscopic conductor (in a given time) should satisfy, for a classical local theory, an inequality.

The paper is organized as follows: In the following section we motivate our approach to the problem, derive the CH inequality, and express the joint probabilities needed in the CH inequality in terms of the scattering properties of the mesoscopic conductor. Section III is devoted to the discussion of the results. We first consider the idealized situation where an incoming flux of fully entangled electrons is injected into the mesoscopic region. Then we move on to analyze actual setups. We consider the case where entanglement is produced by Andreev reflection. However, interacting electrons are not necessary to have an entangled state. Indeed we show that a three terminal normal device is enough to lead to violation of the CH inequality. In the last section we present the conclusions and a brief summary of this work.

## II. CH INEQUALITY FOR THE FULL COUNTING STATISTICS

As mentioned in the Introduction, during the last few years Bell-like inequalities have been proposed to study entanglement in solid-state devices. Very recently, in Ref. 15 it has been shown that zero-frequency current cross correlations, in the tunneling limit, can be used to formulate a Bell inequality. The same authors, in Ref. 30, have shown that such a result can be extended to arbitrary tunneling rates, since a pair of orbitally entangled electrons is postselected by the measurement. In this paper we take a different route by resorting to electron full counting statistics (FCS) for analyzing electronic entanglement. FCS refers to the probability that a given number of electrons has traversed, in a time *t*, a mesoscopic conductor. In the long time limit the first and the second moment of the probability distribution are related to the average current and noise, respectively.

In its original version,[27] the Bell inequality was derived for dichotomic variables. Here we consider the more general formulation proposed by Clauser and Horne.[33] To this aim, we consider the idealized setup, illustrated in Fig. 1, which consists of the following parts. On the left we place an entangler that produces pairs of electrons in a spin-entangled state. Each electron propagates, respectively, into leads 3 and 4 in a superposition of spin states $\uparrow$ and $\downarrow$. (In Sec. III two different situations for the implementation of the entangler are discussed.) Two conductors, characterized by some scattering matrix, connect the terminals 3 and 4 of the entangler with the exit leads 1 and 2 so as to carry the two particles belonging to each pair into two different spatially separated reservoirs. The electron counting is performed in leads 1 and 2 for electrons with spin aligned along the local spin-quantization axis at angles $\theta_1$ and $\theta_2$. Detection is realized by means of spin selective counters, i.e., by counting electrons with the projection of the spin along a given local quantization axis. In analogy with the optical case we say that the analyzer is not present when the electron counting is spin insensitive (electrons are counted irrespective of their spin direction). Since we assume no backscattering from counters to the entangler, the particles which are not counted are lost and hence there is no communication between the two detectors. In the case where only two entangled electrons are injected, we find a situation similar to that with photons. More generally, we discuss the case where a large number of electrons are injected, finding that the CH inequality is violated only when a "coincidence measurement" is performed. In Sec. II A we present the derivation of the CH inequality for the FCS and in Sec. II B we resume, for completeness, the relation between FCS and the scattering matrix *S*.

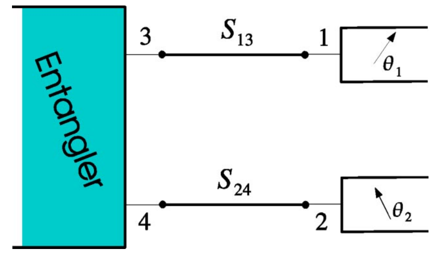


FIG. 1. (Color online) Idealized setup for testing the CH inequality for electrons in a solid-state environment. It consists of two parts: an entangler (shaded block) that produces pairs of spin-entangled electrons exiting from terminals 3 and 4. These terminals are connected to leads 1 and 2 through two conductors described by scattering matrices $S_{13}$ and $S_{24}$. Electron counting is performed in leads 1 and 2 along the local spin-quantization axis oriented at angles $\theta_1$ and $\theta_2$.

### A. Derivation of the CH inequality

The basic object for the formulation of the CH inequality is the joint probability $P(Q_1,Q_2)$ for transferring a number of $Q_1$ and $Q_2$ electronic charges into leads 1 and 2 over an observation time *t*. We follow closely the derivation given in Ref. 34. Our starting point is the following algebraic inequality

$$-1 \leq xy - xy' + x'y + x'y' - x' - y \leq 0, \tag{1}$$

which holds for any variable $0 \leq x,y,x',y' \leq 1$. Let us now introduce explicitly a set of hidden variables $\tau$ which take values in a space $\mathcal{T}$. We assume that the incoming entangled electron states are described by $\tau$ in all the details necessary to determine the probability distributions $P(Q_\alpha,\tau)$ for transferring a number of $Q_\alpha$ electronic charges into lead $\alpha = 1,2$. By imposing that the hidden variable theory is local, it follows that the joint probability can be expressed in the following form:

$$P(Q_1,Q_2) = \int_{\mathcal{T}} \mathcal{M}(\tau) P(Q_1,\tau) P(Q_2,\tau) d\tau, \tag{2}$$

where $\mathcal{M}(\tau)d\tau$ defines a probability measure on the space $\mathcal{T}$. The physical meaning of Eq. (2) is straightforward: it states that the probability distribution on lead $\alpha$ does not depend on the probability distribution on the lead $\beta$.

We now introduce $P^{\theta_1,\theta_2}(Q_1,Q_2)$ as the joint probability for transferring $Q_1$ and $Q_2$ electronic charges when both analyzers are present, while $P^{\theta_1,-}(Q_1,Q_2)$ and $P^{-,\theta_2}(Q_1,Q_2)$ are the corresponding joint probabilities when one of the two analyzers is removed. If the condition

$$P^{\theta_\alpha}(Q_\alpha,\tau)\leqslant P(Q_\alpha,\tau) \tag{3}$$

(known as *no-enhancement assumption*) is verified, it is possible to identify the variables appearing in Eq. (1) as follows:

$$x=\frac{P^{\theta_1}(Q_1,\tau)}{P(Q_1,\tau)},\quad y=\frac{P^{\theta_2}(Q_2,\tau)}{P(Q_2,\tau)},$$

$$x'=\frac{P^{\theta'_1}(Q_1,\tau)}{P(Q_1,\tau)},\quad y'=\frac{P^{\theta'_2}(Q_2,\tau)}{P(Q_2,\tau)}, \tag{4}$$

$P^{\theta}(Q_\alpha,\tau)$ being the single terminal probability distribution in the presence of an analyzer. Equation (1) can then be rewritten in terms of probabilities by multiplying each side of the equation by $P(Q_1,\tau)P(Q_2,\tau)\mathcal{M}(\tau)d\tau$ and integrating over the space $\mathcal{T}$. Finally the following inequality is obtained:

$$\begin{aligned}\mathcal{S}_{CH}=&P^{\theta_1,\theta_2}(Q_1,Q_2)-P^{\theta_1,\theta'_2}(Q_1,Q_2)+P^{\theta'_1,\theta_2}(Q_1,Q_2)\\&+P^{\theta'_1,\theta'_2}(Q_1,Q_2)-P^{\theta'_1,-}(Q_1,Q_2)\\&-P^{-,\theta_2}(Q_1,Q_2)\leqslant 0.\end{aligned} \tag{5}$$

Equation (5) is the CH inequality for the full counting statistics,[35] holding for all values of $Q_1$ and $Q_2$ which satisfy the no-enhancement assumption. We stress that the no-enhancement assumption, upon which Eq. (5) is based, is not satisfied, in general, like its optical version. The quantities that we have to compare are probability distributions, so that Eq. (3) must be checked over the whole range of $Q$. For a fixed time $t$ and a given mesoscopic system, hence for a given scattering matrix and incident particle state, the no-enhancement assumption is valid only in some range of values of $Q$. In particular, different sets of system parameters correspond to different such ranges. The quantity $\mathcal{S}_{CH}$ in Eq. (5) depends on $Q_1$ and $Q_2$ so that the possible violation, or the extent of it, also depends on $Q_1$ and $Q_2$. Given a certain average number $M$ of entangled pairs that have being injected in the time $t$, one can look for the maximum violation as a function of the transmitted charges $Q_1$ and $Q_2$.

### B. Scattering approach to the full counting statistics

The joint probabilities appearing in Eq. (5) can be determined once the scattering matrix $S$ of the mesoscopic conductor is known. The FCS in electronic systems was first introduced by Levitov *et al.* in Refs. 36 and 37 in the context of the scattering theory and later on the Keldysh Green function method[38] to FCS was developed in Ref. 39 (for a review see Ref. 40). In this paragraph we briefly describe how the FCS is formulated for a mesoscopic conductor in the scattering approach. Within this framework, the transport properties of a metallic phase-coherent structure attached to $n$ reservoirs are determined by the matrix $S$ of scattering amplitudes.[41] Such amplitudes are defined through the scattering states describing particles propagating through the leads. For one-dimensional conductors, for example, the scattering state arising from a unitary flux of particles at energy $E$ originating in the $i$th reservoir reads

$$\varphi_i(x)=\frac{e^{ik_i(E)x}+r_i(E)e^{-ik_i(E)x}}{\sqrt{hv_i(E)}} \tag{6}$$

for the $i$th lead, and

$$\varphi_j(x)=\frac{t_{ji}(E)e^{-ik_j(E)x}}{\sqrt{hv_j(E)}}, \tag{7}$$

for the $j$th lead, with $j\neq i$. Here $r_i(E)$ is the reflection amplitude for particles at energy $E$, wave vector $k_i(E)$, and group velocity $v_i(E)$ and $t_{ji}(E)$ is the transmission amplitude from lead $i$ to lead $j$. Note that $|r_i|^2$ is the probability for a particle to reflect back into the $i$th lead and $|t_{ji}|^2$ is the probability for the transmission of a particle from lead $i$ to lead $j$. In the second quantization formalism, the field operator $\hat{\psi}_{j\sigma}(x,t)$ for spin $\sigma$ particles in lead $j$ is built from scattering states and it is defined as

$$\hat{\psi}_{j\sigma}(x,t)=\int dE\ \frac{e^{-iEt/\hbar}}{\sqrt{hv_j(E)}}[\hat{a}_{j\sigma}(E)e^{ik_jx}+\hat{\phi}_{j\sigma}(E)e^{-ik_jx}], \tag{8}$$

where $\hat{a}_{j\sigma}(E)[\hat{\phi}_{j\sigma}(E)]$ is the destruction operator for incoming (outgoing) particles at energy $E$ with spin $\sigma$ in lead $j$. These operators are linked by the equation

$$\begin{pmatrix}\hat{\phi}_{1\uparrow}\\ \hat{\phi}_{1\downarrow}\\ \hat{\phi}_{2\uparrow}\\ \vdots\end{pmatrix}=S\begin{pmatrix}\hat{a}_{1\uparrow}\\ \hat{a}_{1\downarrow}\\ \hat{a}_{2\uparrow}\\ \vdots\end{pmatrix} \tag{9}$$

and obey anticommutation relations

$$\{\hat{a}^{\dagger}_{i\sigma}(E),\ \hat{a}_{j\sigma'}(E')\}=\delta_{i,j}\delta_{\sigma,\sigma'}\delta(E-E'). \tag{10}$$

In the case of two- and three-dimensional leads one can separate longitudinal and transverse particle motion. Since the transverse motion is quantized, the wave function relative to the plane perpendicular to the direction of transport is characterized by a set of quantum numbers which identifies the channels of the lead. Such channels are referred to as open when the corresponding longitudinal wave vectors are real, since they correspond to propagating modes. Note that the case of a single open channel corresponds to a one-dimensional lead.

Let us now turn our attention to the probability distribution for the transfer of charges. Following Ref. 42, within the scattering approach the characteristic function of the probability distribution for the transfer of particles in a structure attached to $n$ leads at a given energy $E$ can be written as

$$\chi_E(\vec{\lambda}_\uparrow,\vec{\lambda}_\downarrow)=\left\langle \prod_{j=1,n} e^{i\lambda_{j\uparrow}\hat{N}_I^{j\uparrow}}e^{\lambda_{j\downarrow}\hat{N}_I^{j\downarrow}}\prod_{j=1,n} e^{-i\lambda_{j\uparrow}\hat{N}_O^{j\uparrow}}e^{-i\lambda_{j\downarrow}\hat{N}_O^{j\downarrow}}\right\rangle, \tag{11}$$

where the brackets $\langle\cdots\rangle$ stand for the quantum statistical average over the thermal distributions in the leads. Assuming a single channel per lead, $\hat{N}_{I(O)}^{j\sigma}$ is the number operator for incoming (outgoing) particles with spin $\sigma$ in lead $j$ and $\vec{\lambda}_\uparrow$, $\vec{\lambda}_\downarrow$ are vectors of $n$ real numbers, one for each open channel. In terms of incoming (outgoing) creation operator the number operators can be expressed as follows:

$$\hat{N}_I^{j\sigma}=\hat{a}_{j\sigma}^\dagger\hat{a}_{j\sigma}, \quad \hat{N}_O^{j\sigma}=\hat{\phi}_{j\sigma}^\dagger\hat{\phi}_{j\sigma}. \tag{12}$$

Equation (11) can also be recasted in the form[36]

$$\chi_E(\vec{\lambda}_\uparrow,\vec{\lambda}_\downarrow)=\det(\mathbb{I}-n_E+n_E \;\; S^\dagger\Lambda^\dagger \;\; S \;\; \Lambda), \tag{13}$$

where $\mathbb{I}$ is the unit matrix, $n_E$ is the diagonal matrix of Fermi distribution functions $f_j(E)$ for particles in the reservoir $j$ and defined as $(n_E)_{j\sigma,j\sigma}=f_j(E)$, whereas $\Lambda$ is a diagonal matrix defined as: $(\Lambda)_{j\sigma,j\sigma}=\exp(i\lambda_{j\sigma})$. For long measurement times $t$ the total characteristic function $\chi$ is the product of contributions from different energies, so that

$$\chi(\vec{\lambda}_\uparrow,\vec{\lambda}_\downarrow)=\exp\left(\frac{t}{h}\int dE\,\ln\chi_E(\vec{\lambda}_\uparrow,\vec{\lambda}_\downarrow)\right). \tag{14}$$

At zero temperature, the statistical average over the Fermi distribution function in Eq. (11) simplifies to the expectation value calculated on the state $|\psi\rangle$ containing two electrons of both spin species for each channel of a given lead up to the energy corresponding to the chemical potential of such lead. Furthermore, in the limit of a small bias voltage $V$ applied between the reservoirs, the argument of the integral is energy independent so that Eq. (14) can be approximated to

$$\chi(\vec{\lambda}_\uparrow,\vec{\lambda}_\downarrow)\simeq[\chi_0(\vec{\lambda}_\uparrow,\vec{\lambda}_\downarrow)]^M, \tag{15}$$

where only the zero-energy characteristic function appears and $M=eVt/h$ is the average number of injected particles. The joint probability distribution for transferring $Q_{1\sigma}$ spin-$\sigma$ electrons in lead 1, $Q_{2\sigma}$ spin-$\sigma$ electrons in lead 2, etc., is related to the characteristic function by the relation (we assume that no polarizers are present)

$$P(Q_{1\uparrow},Q_{1\downarrow},Q_{2\uparrow},\ldots)=\frac{1}{(2\pi)^{2n}}\int_{-\pi}^{+\pi}d\lambda_{1\uparrow}d\lambda_{1\downarrow}d\lambda_{2\uparrow}\cdots\chi(\vec{\lambda}_\uparrow,\vec{\lambda}_\downarrow)\times e^{i\vec{\lambda}_\uparrow\cdot\vec{Q}_\uparrow}e^{i\vec{\lambda}_\downarrow\cdot\vec{Q}_\downarrow}. \tag{16}$$

In the rest of the paper we will consider systems where only two counting terminals are present. In particular, while the counting terminals are kept at the lowest chemical potential, all other terminals are biased at chemical potential $eV$. For later convenience, we write down the most general expression for the characteristic function when spin-$\sigma$ electrons are counted in lead 1 and spin-$\sigma'$ electrons are counted in lead 2:

$$\chi_E(\lambda_{1\sigma},\lambda_{2\sigma'})=1+(e^{-i\lambda_{1\sigma}}-1)\langle\hat{N}_O^{1\sigma}\rangle+(e^{-i\lambda_{2\sigma'}}-1)\times\langle\hat{N}_O^{2\sigma'}\rangle+(e^{-i\lambda_{1\sigma}}-1)(e^{-i\lambda_{2\sigma'}}-1)\times\langle\hat{N}_O^{1\sigma}\hat{N}_O^{2\sigma'}\rangle, \tag{17}$$

in the relevant energy range $0<E<eV$. The parameters $\lambda$ corresponding to all others terminals are set to zero.

Using Eqs. (15), (16), and (17), at zero temperature, one can calculate the single terminal probability distribution

$$P(Q_{1\sigma})=\binom{M}{Q_{1\sigma}}[1-\langle\psi|\hat{N}_O^{1\sigma}|\psi\rangle]^{M-Q_{1\sigma}}\langle\psi|\hat{N}_O^{1\sigma}|\psi\rangle^{Q_{1\sigma}} \tag{18}$$

and the joint probability distribution

$$P(Q_{1\sigma},Q_{2\sigma'})=\sum_{k=\max[M-Q_{1\sigma},M-Q_{2\sigma'}]}^{(M-Q_{1\sigma})+(M-Q_{2\sigma'})}A^{2M-Q_{1\sigma}-Q_{2\sigma'}-k}\times B^{Q_{1\sigma}-M+k}\;\;C_{2\sigma'}^{k-M+Q}\langle\psi|\hat{N}_O^{1\sigma}\hat{N}_O^{2\sigma'}|\psi\rangle^{M-k}\times f(M,Q_{1\sigma},Q_{2\sigma'},k), \tag{19}$$

where $A=1-\langle\psi|\hat{N}_O^{1\sigma}|\psi\rangle-\langle\psi|\hat{N}_O^{2\sigma'}|\psi\rangle+\langle\psi|\hat{N}_O^{1\sigma}\hat{N}_O^{2\sigma'}|\psi\rangle$, $B=\langle\psi|\hat{N}_O^{1\sigma}(1-\hat{N}_O^{2\sigma'})|\psi\rangle$, $C=\langle\psi|(1-\hat{N}_O^{1\sigma})\hat{N}_O^{2\sigma'}|\psi\rangle$, and $f(M,Q_{1\sigma},Q_{2\sigma'},k)=M!/[(k-M+Q_{2\sigma'})!(2M-k-Q_{1\sigma}-Q_{2\sigma'})!]$. In doing so we have written the expressions for the probability distributions in terms of the expectation values of "outgoing" number operators. For $Q_{1\sigma}=Q_{2\sigma'}=M$, Eq. (19) reduces to

$$P(Q_{1\sigma}=M,Q_{2\sigma'}=M)=\langle\psi|\hat{N}_O^{1\sigma}\hat{N}_O^{2\sigma'}|\psi\rangle^M. \tag{20}$$

When both spin species are counted in one of the terminals the characteristic function is different from the one given in Eq. (17). In particular, the characteristic function for counting both spins in terminal 1 reads

$$\chi_E(\lambda_1,\lambda_{2\sigma'})=1+(e^{-i\lambda_1}-1)\langle(\hat{N}_O^{1\uparrow}+\hat{N}_O^{1\downarrow})\rangle+(e^{-i\lambda_{2\sigma'}}-1)\times\langle\hat{N}_O^{2\sigma'}\rangle+(e^{-i\lambda_1}-1)(e^{-i\lambda_{2\sigma'}}-1)\times\langle(\hat{N}_O^{1\uparrow}+\hat{N}_O^{1\downarrow})\hat{N}_O^{2\sigma'}\rangle+(e^{-i\lambda_1}-1)^2\langle\hat{N}_O^{1\uparrow}\hat{N}_O^{1\downarrow}\rangle+(e^{-i\lambda_1}-1)^2(e^{-i\lambda_{2\sigma'}}-1)\langle\hat{N}_O^{1\uparrow}\hat{N}_O^{1\downarrow}\hat{N}_O^{2\sigma'}\rangle, \tag{21}$$

where we have set $\lambda_{1\uparrow}=\lambda_{1\downarrow}\equiv\lambda_1$. The expression for the joint probability distribution is, in general, complicated, as one can see in the Appendix where such expressions for different systems are reported.

## III. RESULTS

The inequality presented in Eq. (5) can be tested in various multiterminal mesoscopic conductors. In this section we present several geometries that can be experimentally realized. In order to get acquainted with the informations that can be retrieved from Eq. (5) we start from an ideal case in which the entangled pair is generated by some *entangler* in the same spirit as in the works of Refs. 9 and 10. In Sec. III B we analyze the role of superconductivity in creating spin singlets. In Sec. III C we shall demonstrate that a normal beam splitter in the absence of interaction is enough to generate entangled pairs of electrons, therefore constituting a simple realization of an entangler.

### A. Entangled electrons

In the setup depicted in Fig. 1 we assume the existence of an entangler that produces electron pairs in the Bell state

$$|\psi\rangle=\frac{1}{\sqrt{2}}[a^{\dagger}_{3\uparrow}(E)a^{\dagger}_{4\downarrow}(E)\pm a^{\dagger}_{3\downarrow}(E)a^{\dagger}_{4\uparrow}(E)]|0\rangle, \quad (22)$$

of spin triplet (upper sign) or spin singlet (lower sign) in the energy range $0<E<eV$. These electrons propagate through the conductors which connect terminals 3 and 4 with leads 1 and 2, as though terminals 3 and 4 were kept at a potential $eV$ with respect to 1 and 2. Our aim is to test the violation of the CH inequality given in Eq. (5) for such maximally entangled states.

When the angles $\theta_1$ and $\theta_2$ are parallel to each other, the scattering matrix of the two conductors, in the absence of spin mixing processes, can be written as

$$S=\begin{pmatrix} \hat{S}_{13} & 0 \\ 0 & \hat{S}_{24} \end{pmatrix}, \quad (23)$$

where

$$\hat{S}_{13}=\begin{pmatrix} \check{r}_3 & \check{t}_{31} \\ \check{t}_{13} & \check{r}_1 \end{pmatrix}=\begin{pmatrix} r_{3\uparrow} & 0 & t_{31\uparrow} & 0 \\ 0 & r_{3\downarrow} & 0 & t_{31\downarrow} \\ t_{13\uparrow} & 0 & r_{1\uparrow} & 0 \\ 0 & t_{13\downarrow} & 0 & r_{1\downarrow} \end{pmatrix}. \quad (24)$$

Here $r_{j\sigma}$ ($t_{ij\sigma}$) is the probability amplitude for an incoming particle with spin $\sigma$ from lead $j$ to be reflected (transmitted in lead $i$). For a normal-metallic wire we set $t_{ij\uparrow}=t_{ij\downarrow}=\sqrt{T}$, $t_{ji\uparrow}=t_{ji\downarrow}=-\sqrt{T}$, and $r_{j\uparrow}=r_{j\downarrow}=\sqrt{1-T}$, where $T$ is the transmission probability. The expression for $\hat{S}_{24}$ is written analogously. For simplicity we will assume that $\hat{S}_{13}$ and $\hat{S}_{24}$ are equal. The general scattering matrix relative to noncollinear angles is obtained from $S$ by rotating the spin quantization axis independently in the two conductors (note that this is possible because the two wires are decoupled). The "rotated" $S$ matrix is obtained[43] by the transformation $S_{\theta_1,\theta_2}=\mathcal{U}S\mathcal{U}^{\dagger}$, where $\mathcal{U}$ is the rotation matrix given by

$$\mathcal{U}=\begin{pmatrix} U_{\theta_1} & 0 & 0 & 0 \\ 0 & \mathbb{I} & 0 & 0 \\ 0 & 0 & U_{\theta_2} & 0 \\ 0 & 0 & 0 & \mathbb{I} \end{pmatrix}, \quad (25)$$

where

$$U_{\theta}=\begin{pmatrix} \cos\frac{\theta}{2} & \sin\frac{\theta}{2} \\ -\sin\frac{\theta}{2} & \cos\frac{\theta}{2} \end{pmatrix}. \quad (26)$$

The probability distributions are now given by the expressions in Eq. (18) and Eq. (19) where the state $|\psi\rangle$ is given by Eq. (22). In the case where both analyzers are present we set $\sigma=\sigma'=\uparrow$. The probability distribution when one of the analyzers is removed also possesses the structure of Eq. (19) since, in this case, the correlators $\langle\hat{N}^{1\uparrow}_{\mathrm{O}}\hat{N}^{1\downarrow}_{\mathrm{O}}\rangle$ and $\langle\hat{N}^{1\uparrow}_{\mathrm{O}}\hat{N}^{1\downarrow}_{\mathrm{O}}\hat{N}^{2\uparrow}_{\mathrm{O}}\rangle$ appearing in Eq. (21) vanish. In particular when, for example, the upper analyzer in Fig. 1 is removed we need to replace $\hat{N}^{1\sigma}_{\mathrm{O}}$ with $\hat{N}^{1\uparrow}_{\mathrm{O}}+\hat{N}^{1\uparrow}_{\mathrm{O}}$ and $\hat{N}^{2\sigma'}_{\mathrm{O}}$ with $\hat{N}^{2\uparrow}_{\mathrm{O}}$. For the other correlators one gets

$$\langle\psi|\hat{N}^{1\uparrow}_{\mathrm{O}}|\psi\rangle=\langle\psi|\hat{N}^{2\uparrow}_{\mathrm{O}}|\psi\rangle=\frac{T}{2}, \quad (27)$$

$$\langle\psi|\hat{N}^{1\downarrow}_{\mathrm{O}}|\psi\rangle=\frac{T}{2}, \quad (28)$$

$$\langle\psi|\hat{N}^{1\uparrow}_{\mathrm{O}}\hat{N}^{2\uparrow}_{\mathrm{O}}|\psi\rangle=\frac{T^2}{2}\sin^2\left(\frac{\theta_1\pm\theta_2}{2}\right), \quad (29)$$

and

$$\langle\psi|\hat{N}^{1\downarrow}_{\mathrm{O}}\hat{N}^{2\uparrow}_{\mathrm{O}}|\psi\rangle=\frac{T^2}{2}\cos^2\left(\frac{\theta_1\pm\theta_2}{2}\right). \quad (30)$$

For the single terminal probability distributions in leads $i=1,2$ we get, in the presence and in the absence of an analyzer, respectively,

$$P^{\theta_i}(Q_i)=\binom{M}{Q_i}\left(\frac{T}{2}\right)^{Q_i}\left(1-\frac{T}{2}\right)^{M-Q_i}, \quad (31)$$

$$P(Q_i)=\binom{M}{Q_i}(T)^{Q_i}(1-T)^{M-Q_i}, \quad (32)$$

so that the no-enhancement assumption reads

$$\left(1-\frac{T}{2}\right)^{(M-Q_i)}\left(\frac{1}{2}\right)^{Q_i}\leqslant(1-T)^{(M-Q_i)}, \quad i=1,2. \quad (33)$$

Note that the probabilities in Eqs. (31) and (32) do not depend on the angles $\theta_1$ and $\theta_2$ because the expectation values in Eqs. (27) and (28) are invariant under spin rotation. As a consequence, the effect of the analyzer is equivalent to a reduction of the transmission probability $T$ by a factor of 2, resulting in a shift of the maximum of the distribution. From Eq. (33) it follows that, for a given number $M=eVt/h$ of entangled pairs generated by the entangler, the no enhancement assumption holds only for certain values of $T$ and of $Q_i$. Thus the CH inequality of Eq. (5) can be tested for violation only for appropriate values of $M$, $T$ and $Q_1$ or $Q_2$. For example, for a given observation time $t$ (i.e., a given $M$)

and a given value of $Q$, CH inequality can be tested only for transmission $T$ less than a maximum value given by the expression

$$T_{\max}=\frac{2^{Q_i/(M-Q_i)}-1}{2^{Q_i/(M-Q_i)}-\frac{1}{2}}. \tag{34}$$

At the edge of the distribution ($Q_i=M$) the no-enhancement assumption is satisfied for every $T$. The window of allowed $Q_i$ values where the no-enhancement assumption is satisfied gets wider on approaching the tunneling limit. For large $M$, $T_{\max}\simeq 2(\ln 2)Q_i/M$. The previous inequality can be also interpreted as a limit for the allowed measuring time given a setup at disposal. Alternatively, given a certain transmission, the no-enhancement assumption is verified for points of the distribution such that

$$\frac{Q_i}{M}\geqslant\frac{\ln\dfrac{1-T/2}{1-T}}{\ln 2+\ln\dfrac{1-T/2}{1-T}}. \tag{35}$$

The various probabilities needed to define $\mathcal{S}_{CH}$ are collected in the Appendix. However, it is useful to note here that the joint probabilities with a single analyzer are factorized:

$$P^{\theta_1,-}(Q_1,Q_2)=P^{\theta_1}(Q_1)P(Q_2),$$
$$P^{-,\theta_2}(Q_1,Q_2)=P(Q_1)P^{\theta_2}(Q_2), \tag{36}$$

while joint probabilities with two analyzers are not factorized. Furthermore, all such probabilities have a common factor, $T^{Q_1+Q_2}/2^M$, which leads to an exponential suppression for large $M$ and $Q_1+Q_2$. We shall address the question of whether this also produces a suppression of $\mathcal{S}_{CH}$ in case of violation.

Let us now analyze the possibility of violation of the CH inequality for different values of $Q_1$ and $Q_2$. First consider the situation where the entangler emits a single entangled pair of electrons in which case $P^{\theta_1,\theta_2}(1,1)=\langle\psi|\hat{N}_O^{1\uparrow}\hat{N}_O^{2\uparrow}|\psi\rangle$, $P^{-,\theta_2}(1,1)=\langle\psi|(\hat{N}_O^{1\uparrow}+\hat{N}_O^{1\downarrow})\hat{N}_O^{2\uparrow}|\psi\rangle$, and $P^{\theta_1,-}(1,1)=\langle\psi|\hat{N}_O^{1\uparrow}(\hat{N}_O^{2\uparrow}+\hat{N}_O^{2\uparrow})|\psi\rangle$. We find that the CH inequality is maximally violated for the following choice of angles: $\theta_2-\theta_1=\theta_2'-\theta_1'=3\pi/4$. More precisely, we obtain

$$\mathcal{S}_{CH}=T^2\frac{\sqrt{2}-1}{2}, \tag{37}$$

which is equal to the result obtain for an entangled pair of photons,[34] where $T$ plays the role of the quantum efficiency of the photon detectors. In the more general case of $Q_1=Q_2=M$, for $M\gg 1$, we have

$$P^{\theta_1,\theta_2}(M,M)=\frac{T^{2M}}{2^M}\left[\sin^2\left(\frac{\theta_1\pm\theta_2}{2}\right)\right]^M,$$

$$P^{\theta_1,-}(M,M)=P^{-,\theta_2}(M,M)=\frac{T^{2M}}{2^M} \tag{38}$$

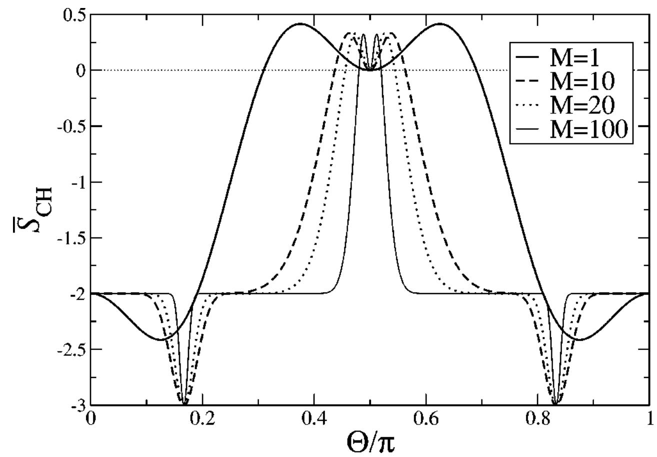


FIG. 2. The quantity $\bar{\mathcal{S}}_{CH}=\mathcal{S}_{CH}/(T^{2M}/2^M)$ is plotted as a function of the angle $\Theta$ for different numbers $M$ of injected entangled pairs by the entangler. The range of angles relative to positive values shrinks with increasing $M$, while the value of the maximum slightly decreases.

so that the no-enhancement assumption is always satisfied and the quantity $\mathcal{S}_{CH}$ can be easily evaluated:

$$\mathcal{S}_{CH}=\frac{T^{2M}}{2^M}\left[\sin^{2M}\frac{\theta_1\pm\theta_2}{2}-\sin^{2M}\frac{\theta_1\pm\theta_2'}{2}+\sin^{2M}\frac{\theta_1'\pm\theta_2}{2}+\sin^{2M}\frac{\theta_1'\pm\theta_2'}{2}-2\right]. \tag{39}$$

The rotational invariance makes $P^{\theta_1,-}$ and $P^{-,\theta_2}$ independent of angles, and $P^{\theta_1,\theta_2}$ dependent on the angles through $(\theta_1\pm\theta_2)/2$. This allows us, without loss of generality, to define an angle $\Theta$ such that $2\Theta=\theta_1\pm\theta_2=\theta_1'\pm\theta_2=\theta_1'\pm\theta_2'=(\theta_1\pm\theta_2')/3$. As a result Eq. (5) takes the form

$$\mathcal{S}_{CH}=3P_{1,2}^{\Theta}(Q_1,Q_2)-P_{1,2}^{3\Theta}(Q_1,Q_2)-P_{1,-}(Q_1,Q_2)-P_{-,2}(Q_1,Q_2)\leqslant 0, \tag{40}$$

where $P_{1,2}^{\Theta}=P^{\theta_1,\theta_2}$ and $P_{1,-}=P^{\theta_1,-}$. It is useful to define the reduced quantity $\bar{\mathcal{S}}_{CH}=\mathcal{S}_{CH}/(T^{2M}/2^M)$ which is plotted in Fig. 2 as a function of $\Theta$ for different values of $M$ [note that since $P^{\theta_1,-}(M,M)=(T^{2M}/2^M)$, $\bar{\mathcal{S}}_{CH}$ is nothing but $\mathcal{S}_{CH}/P^{\theta_1,-}(M,M)$]. The violation occurs for every value of $M$ in a range of angles around $\Theta=\pi/2$ (note that $\mathcal{S}_{CH}$ is symmetric with respect to $\pi/2$). The range of angles for which $\bar{\mathcal{S}}_{CH}$ is positive shrinks with increasing $M$, while the maximum value of $\bar{\mathcal{S}}_{CH}$ decreases very weakly with $M$ (more precisely, $\bar{\mathcal{S}}_{CH}^{\max}\propto 1/M$). This means that the effect of the factor $T^{2M}/2^M$ on the value of $\mathcal{S}_{CH}$ is exponentially strong, making the violation of the CH inequality exponentially difficult to detect for large $M$ and $Q_1=Q_2=M$. The weakening of the violation is mainly due to the suppression of the joint probabilities. As we shall show later, by optimizing all the parameters it is yet possible to eliminate this exponential suppression.

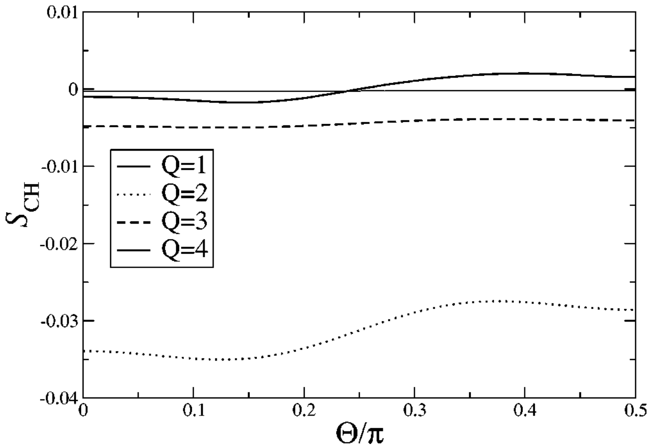


FIG. 3. The quantity $\mathcal{S}_{CH}$ is plotted as a function of the angle $\Theta$ for $M=20$ and $T=0.069\,17$, which corresponds to the highest value allowed by the no-enhancement assumption for $Q=1$. The curves are relative to different values of $Q=[1,4]$. Note that for $Q\geqslant 4$ the variation of $\mathcal{S}_{CH}$ over the whole range of $\Theta$ is small on the scale of the plot. Violations are found only for $Q=1$ and $Q=20$.

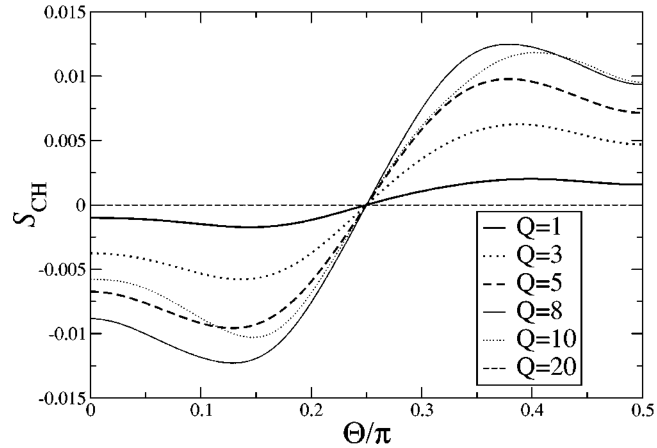


FIG. 4. The quantity $\mathcal{S}_{CH}$ is plotted as a function of the angle $\Theta$ for $M=20$ and $T$ set to the highest value allowed by the no-enhancement assumption, different from each $Q$. The curves are relative to different values of $Q=[1,20]$. The maximum of $\mathcal{S}_{CH}$ increases with $Q$ reaching its largest value for $Q=8$ and decreasing for $Q>8$. Note that the variation of $\mathcal{S}_{CH}$ with $\Theta$ for $Q=20$ it is not appreciable on this scale.

Let us now consider the violation of the CH inequality as a function of the transmitted charges. We notice that the CH inequality is not violated for the off-diagonal terms of the distributions (when $Q_1\neq Q_2$), meaning that one really needs to look at "coincidences." Therefore we discuss the case $Q_1=Q_2\equiv Q<M$ [remember that the no-enhancement assumption is satisfied only for $T\leqslant T_{\max}(Q)$]. In Fig. 3 we plot the quantity $\mathcal{S}_{CH}$ for $M=20$ as a function of $\Theta$ and different values of $Q$. The transmission $T$ is fixed at the highest allowed value by the no-enhancement assumption, which corresponds to the smallest $Q$ considered $T_{\max}(Q=1)=0.069\,17$. Figure 3 shows that the largest positive value of $\mathcal{S}_{CH}$ and the widest range of angles corresponding to positive $\mathcal{S}_{CH}$ occur for $Q=1$, i.e., for a joint probability relative to the detection of a single pair. One should not conclude that, in order to detect the violation of the CH inequality, only very small values of the transmitted charge should be taken. We have, in fact, considered $T=T_{\max}$ relative to $Q=1$ and the maximum violation, for given $M$ and $Q$, always occurs at $T=T_{\max}$. In order to get the largest violation of the CH inequality at a given $M$ and $Q$ one could, in principle, choose the highest allowed value of $T$ for each value of $Q[T=T_{\max}(Q)]$. We show in Fig. 4 the corresponding plot, to be compared with Fig. 3. For every $Q<M$ the violation occurs in the same range of angles, namely $\pi/4\leqslant\Theta\leqslant\pi/2$, because of the following properties of the joint probability distributions: $P_{1,2}^{\Theta}(Q_1,Q_2)=P_{1,2}^{3\Theta}(Q_1,Q_2)=P_{1,-}(Q_1,Q_2)$ for $\Theta=\pi/4$. This implies that $\mathcal{S}_{CH}(\Theta=\pi/4)=0$, and $P_{1,2}^{\Theta}(Q_1,Q_2)\geqslant P_{1,2}^{3\Theta}(Q_1,Q_2),P_{1,-}^{\Theta}(Q_1,Q_2),P_{-,2}^{\Theta}(Q_1,Q_2)$ for $\pi/4\leqslant\Theta\leqslant\pi/2$. Furthermore, in this specific case of $M=20$, we find that the maximum values of $S$ occurs at $Q=8$.

In Fig. 5 we plot the maximum value of $S$, with respect to $\Theta$ and $T$, as a function of $Q$ for different values of $M$. Several observations are in order. For increasing $M$, the position of the maximum, $Q_{\max}$, is very weakly dependent on $M$. Remarkably, the value of the maximum of the curves does not decrease exponentially, but rather as $1/M^2$. Despite the exponential suppression of the joint probability with $M$, the extent of the maximal violation scales with $M$ much slowly (polynomially).

It may be useful to look at the same situation from a different perspective. Given a certain transmission $T$ (i.e., fixing the transport properties of the conductors) we want to find when the CH inequality is maximally violated. For a given observation time $t$, the no-enhancement assumption, Eq. (34), imposes a minimum value for $Q$. In Fig. 6 we plot the quantity $\mathcal{S}_{CH}$, maximized over the angle $\Theta$ and $Q$, as a function of $T$ for different $M$. The curves are a piecewise increasing function of $T$, where the discontinuities correspond to an increase of the value of $Q$ by one imposed by the no-enhancement assumption. More precisely, when $T$ is in-

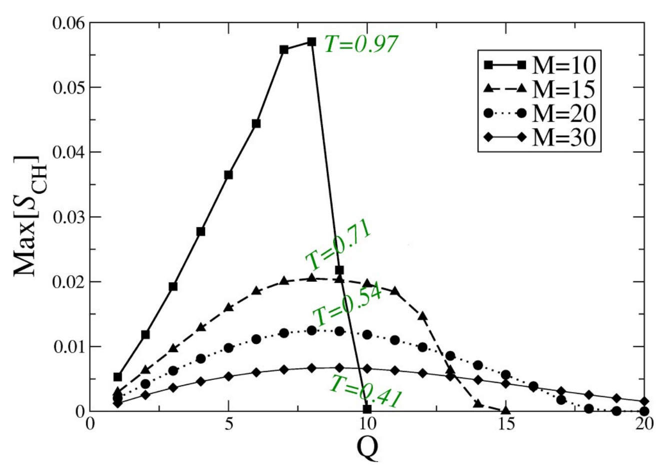


FIG. 5. The maximum value of the quantity $\mathcal{S}_{CH}$, evaluated over angles $\Theta$ and transmission probabilities $T$, is plotted as a function of $Q$. The curves are relative to different values of $M$ ranging from 10 to 30. For points corresponding to the maximum of the curves we indicate the corresponding value of transmission $T$.

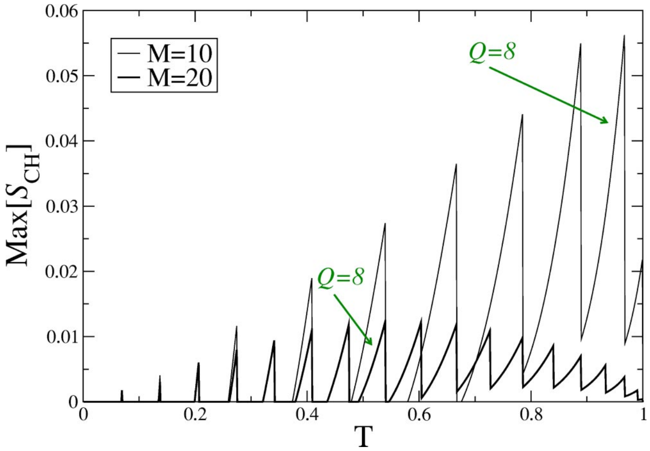


FIG. 6. (Color online) The maximum value of the quantity $\mathcal{S}_{CH}$, evaluated over angles $\Theta$ and number of counted electrons $Q$, is plotted as a function of $T$. Both curves, relative to $M=10$ and $M=20$, exhibit discontinuities which correspond to an increase of the value of $Q$ by 1. This increase is imposed by the no-enhancement assumption, Eq. (35), which depends on the value of $T$. We indicate the value of $Q$ which corresponds to the largest violation.

creased above a threshold for which Eq. (34) is not satisfied, one needs to increase $Q$ by one unit in order for this condition to be recovered. The result of this is a jump in the values of the probabilities that leads to a discontinuity of $\mathcal{S}_{CH}$. Figure 6 allows to choose the best values of $M$ and $Q$ to get the maximum violation.

If the entangler is substituted with a source that emits factorized states, the CH inequality given in Eq. (5) is never violated. In this case, in contrast to Eq. (22), the state emitted by the source reads $|\psi\rangle = a^\dagger_{3\uparrow} a^\dagger_{4\uparrow}|0\rangle$. All the previous calculations can be repeated and we find, as expected, that the characteristic functions factorizes, so that the two terminal joint probability distributions are given by the product of the single terminal probability distributions. To conclude, we wish to mention that the CH inequality, Eq. (5), holds for joint probabilities relative to arbitrary observation time, although the FCS requires long observation time, so that $M \gg 1$.

We are now ready to analyze realistic structures by replacing the shaded block in Fig. 1 (which represents the entangler) with a certain system, and discuss the CH inequality along the lines of Sec. III A.

### B. Superconducting beam splitter

In many proposals superconductivity has been identified as a key ingredient for the creation of entangled pairs of electrons. The idea is to extract the two electrons which compose a Cooper pair (a) pair of spin-entangled electrons) from two spatially separated terminals. We analyze the case of a superconducting beam splitter[44,45] depicted in Fig. 7, which consists of a superconducting lead (with condensate chemical potential equal to $\mu$) in contact with two normal wires. The wires are then connected to two leads attached to reservoirs kept at zero potential. This is basically what is obtained by replacing the entangler of Fig. 1 by a superconducting lead with two terminals.

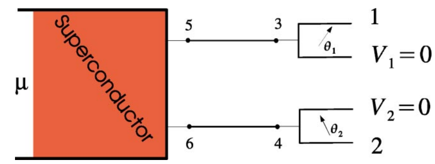


FIG. 7. (Color online) Setup of a realistic system consisting of a superconducting beam splitter (shaded region) for testing the CH inequality. Bold lines represent two conductors of transmission probability $T$. The superconducting condensate electrochemical potential is set to $\mu$, while terminals 1 and 2 are grounded.

The system can be decomposed into two subsystems: on the left-hand side of Fig. 7 we place the superconducting slab attached to two normal terminals (5 and 6) characterized by a reflection amplitudes matrix $R'_s$ defined, in terms of the particle operators, by

$$\hat{\phi}_{j\alpha\sigma}(E) = \sum_{k=5,6} \sum_{\beta=e,h} \sum_{\sigma'=\uparrow,\downarrow} [R'_s(E)]_{j\alpha\sigma,k\beta\sigma'} \; \hat{a}_{k\beta\sigma'}(E). \tag{41}$$

Here $j=5,6$ and the additional indices $\alpha$ and $\beta$ refer to the particle-hole degree of freedom, in particular, $\alpha=e$ for particles and $\alpha=h$ for holes and $[\cdots]_{j\alpha\sigma,k\beta\sigma'}$ represents the specified element of the matrix. Note that $R'_s$ is block diagonal in spin indices so that

$$R'_s = \begin{pmatrix} \mathcal{R}' & 0 \\ 0 & \mathcal{R}' \end{pmatrix} \tag{42}$$

with

$$\begin{pmatrix} \hat{\phi}_{5e\uparrow} \\ \hat{\phi}_{5h\downarrow} \\ \hat{\phi}_{6e\uparrow} \\ \hat{\phi}_{6h\downarrow} \end{pmatrix} = \mathcal{R}' \begin{pmatrix} \hat{a}_{5e\uparrow} \\ \hat{a}_{5h\downarrow} \\ \hat{a}_{6e\uparrow} \\ \hat{a}_{6h\downarrow} \end{pmatrix},$$

$$\mathcal{R}' = \begin{pmatrix} \rho_{ee} & \rho_{ph} & \tau_{ee} & \tau_{eh} \\ \rho_{he} & \rho_{hh} & \tau_{he} & \tau_{hh} \\ \tau'_{ee} & \tau'_{eh} & \rho'_{pp} & \rho'_{eh} \\ \tau'_{he} & \tau'_{hh} & \rho'_{hp} & \rho'_{hh} \end{pmatrix}, \tag{43}$$

where $\rho_{ee}$ ($\rho_{hh}$) is the normal reflection amplitude for particles (holes) in terminal 5, $\rho_{eh}$ ($\rho_{he}$) is the Andreev reflection for a hole to evolve into a particle (particle to evolve into a hole) in terminal 5. $\tau_{ee}$ ($\tau_{hh}$) is the normal transmission amplitude for particles (holes) to be transmitted from terminal 5 to terminal 6, $\tau_{eh}$ ($\tau_{he}$) is the Andreev transmission amplitude for holes (particles) in terminal 5 to be transmitted in terminal 6 as particles (holes). Primed amplitudes refer to reflections occurring in lead 6 and transmissions from lead 6 to lead 5.

On the right-hand side of Fig. 7 we have the subsystem composed of two identical decoupled conductors characterized by the $16\times16$ scattering matrix

$$S_{\rm c}=\begin{pmatrix} R_{\rm c} & T'_{\rm c} \\ T_{\rm c} & R'_{\rm c} \end{pmatrix}. \tag{44}$$

The four submatrices in Eq. (44) are block diagonal in spin space, for example, $R_{\rm c}$ can be written as

$$R_{\rm c}=\begin{pmatrix} R_{\rm c}^{\uparrow} & 0 \\ 0 & R_{\rm c}^{\downarrow}, \end{pmatrix}, \tag{45}$$

where $R_{\rm c}^{\uparrow}$ is a diagonal matrix defined by

$$\begin{pmatrix} \hat{\phi}_{3e\uparrow} \\ \hat{\phi}_{3h\downarrow} \\ \hat{\phi}_{4e\uparrow} \\ \hat{\phi}_{4h\downarrow} \end{pmatrix} = R_{\rm c}^{\uparrow} \begin{pmatrix} \hat{a}_{3e\uparrow} \\ \hat{a}_{3h\downarrow} \\ \hat{a}_{4e\uparrow} \\ \hat{a}_{4h\downarrow} \end{pmatrix},$$

$$R_{\rm c}^{\uparrow}=\begin{pmatrix} r_{3e\uparrow} & 0 & 0 & 0 \\ 0 & r_{3h\downarrow} & 0 & 0 \\ 0 & 0 & r_{4e\uparrow} & 0 \\ 0 & 0 & 0 & r_{4h\downarrow} \end{pmatrix}. \tag{46}$$

$R_{\rm c}^{\downarrow}$ is defined like $R_{\rm c}^{\uparrow}$ exchanging $\uparrow$ with $\downarrow$, whereas $T_{\rm c}^{\sigma}$ is defined similarly to $R_{\rm c}^{\sigma}$ replacing $r_{3\alpha\sigma}$ with $t_{1\alpha\sigma}$ and $r_{4\alpha\sigma}$ with $t_{2\alpha\sigma}$. The matrices $R_{\rm c}'^{\sigma}$ and $T_{\rm c}'^{\sigma}$ are defined analogously using the amplitudes $r_{1\alpha\sigma}$, $r_{2\alpha\sigma}$, $t'_{1\alpha\sigma}$, and $t'_{2\alpha\sigma}$. The spin quantization axis of the two wires can be rotated independently as in Sec. III A by applying the transformation $S_{\theta_1,\theta_2}=\mathcal{U}S_{\rm c}\mathcal{U}^{\dagger}$, where $\mathcal{U}$ is defined in Eq. (25), obtaining the scattering matrix

$$S_{\theta_1,\theta_2}=\begin{pmatrix} \tilde{R}_{\rm c} & \tilde{T}'_{\rm c} \\ \tilde{T}_{\rm c} & \tilde{R}'_{\rm c} \end{pmatrix}. \tag{47}$$

The overall matrix of reflection amplitudes is calculated by composing the scattering matrices relative to the two subsystems,[46]

$$R'_{\rm tot}=\tilde{R}'_{\rm c}+\tilde{T}_{\rm c}[\mathbb{I}-R'_{\rm s}\tilde{R}_{\rm c}]^{-1}R'_{\rm s}\tilde{T}'_{\rm c}, \tag{48}$$

where $R'_{\rm tot}$ is defined by

$$\hat{\phi}_{j\alpha\sigma}(E)=\sum_{k=1,2}\sum_{\beta=e,h}\sum_{\tau=\uparrow,\downarrow}[R'_{\rm tot}(E)]_{j\alpha\sigma,k\beta\tau}\;\hat{a}_{k\beta\tau}(E) \tag{49}$$

with $j$ running from 1 to 2. The characteristic function can now be calculated through Eq. (13) taking $R'_{\rm tot}(E)$ as scattering matrix. In the present case, where superconductivity is present, the diagonal matrix of Fermi distribution functions is defined as $[n_E]_{j\alpha\sigma,j\alpha\sigma}=f_{j\alpha}(E)$, $f_{j\alpha}(E)=\{1+\exp[(E+\alpha\mu)/k_BT]\}^{-1}$ and $[\Lambda]_{j\alpha\sigma,j\alpha\sigma}=\exp(i\alpha\lambda_{j\sigma})$ with $j=1,2$. By choosing $\lambda_{1\downarrow}=\lambda_{2\downarrow}=0$ we achieve the goal of counting excitations with spin-up component. The case where one of the analyzers is removed, for example, in lead 1, is implemented by setting $\lambda_{1\downarrow}=\lambda_{1\uparrow}=\lambda_1$ and $\theta_1=0$, i.e., by counting electrons in lead 1 regardless of their spin.

In the limit of zero temperature and small bias voltage, we only need the scattering amplitudes at the zero energy (Fermi level) so that the overall characteristic function can be approximated like in Eq. (15). We parametrize the matrix $S_{\rm c}$ of the wires as follows: $r_{3e\sigma}=r_{4e\sigma}=\sqrt{1-T}$, $r_{1e\sigma}=r_{2e\sigma}=\sqrt{1-T}$, $t_{1e\sigma}=t_{1e\sigma}=\sqrt{T}$, and $t'_{1e\sigma}=t'_{2e\sigma}=-\sqrt{T}$, where $T$ is the wire transmission probability of the wires. The amplitudes relative to hole degree of freedom are determined from the ones above by making use of the particle-hole symmetry. The no-enhancement assumption can be calculated along the lines of Eqs. (31)–(33) and it is easy to check that for $Q_2=Q_3=M$ it is always satisfied.

Although Andreev processes are fundamental for the injection of Cooper pairs, in the case where Andreev transmissions only are nonzero and $T=1$ the joint probabilities factorize in a trivial way,

$$P^{\theta_1,\theta_2}(Q_1,Q_2)=\delta_{Q_1,2M}\delta_{Q_2,2M},$$

$$P^{\theta_1,-}(Q_1,Q_2)=\delta_{Q_1,2M}\delta_{Q_2,4M}, \tag{50}$$

in such a way that the CH inequality is never violated. This apparent contradiction is due to the fact that in this situation the scattering processes occur with unit probability, so that the condition of locality is fulfilled. Nonlocality can be achieved by imposing $T<1$. In the limit $T\ll 1$ we obtain the probabilities $P^{\theta_1,\theta_2}(Q_1,Q_2)$ and $P^{-,\theta_2}(Q_1,Q_2)$ reported, respectively, in Eqs. (AA5) and (AA6) of the Appendix, which reduce to

$$P^{\theta_1,\theta_2}(M,M)=\left[\frac{2T^2A^6}{[A-T(A-1)]^8}\right]^M\left[\sin^2\left(\frac{\theta_1+\theta_2}{2}\right)\right]^M \tag{51}$$

and

$$P^{-,\theta_2}(M,M)=\left[\frac{2T^2A^6}{[A-T(A-1)]^8}\right]^M \tag{52}$$

for $Q_2=Q_3=M$, with $A=1+\tau_{he}\tau_{he}'^{*}$. Equations (51) and (52) are equal to Eqs. (38), relative to the case of an entangler, once $2T^2A^6/[A-T(A-1)]^8$ is replaced with $T^2/2$. From this follows that superconductivity leads to violation of the CH inequality For $A=2$, i.e., perfect Andreev transmission, the quantity $2T^2A^6/[A-T(A-1)]^8$ tends to $T^2/2$ in the limit $T\to 0$ so that the analysis of Sec. III C relative to the case $Q_1=Q_2=M$ applies also here.

### C. Normal beam splitter

It is interesting to show that, even in the absence of superconductivity, a normal beam splitter leads to violations of the CH inequality. To this aim, we consider a normal beam splitter (shaded block in Fig. 8) in which lead 3 is kept at a potential $eV$ and leads 1 and 2 are grounded so that the same bias voltage is established between 3 and 1, and 3 and 2. The two conductors, which connect the beam splitter to the leads 1 and 2, are assumed to be normal-metallic and perfectly

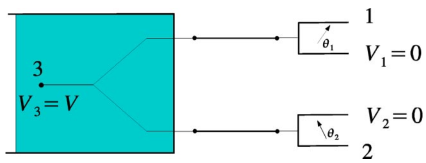


FIG. 8. (Color online) Setup of a realistic system consisting of a normal beam splitter (shaded region) for testing the CH inequality. Bold lines represent two conductors of unit transmission probability. A bias voltage equal to $eV$ is set between terminals 3 and 1 and terminals 3 and 2.

transmissive, so that the $S$ matrix of the system for $\theta_1=\theta_2=0$ is equal to the $S$ matrix of the beam splitter, which reads[47]

$$S=\begin{pmatrix} -(a+b) & \sqrt{\epsilon} & \sqrt{\epsilon} \\ \sqrt{\epsilon} & a & b \\ \sqrt{\epsilon} & b & a \end{pmatrix}. \tag{53}$$

In this parametrization of a symmetric beam splitter $a=\pm(1+\sqrt{1-2\epsilon})/2$, $b=\mp(1-\sqrt{1-2\epsilon})/2$, and $0<\epsilon<1/2$. For arbitrary angles $\theta_1$ and $\theta_2$, the $S$ matrix is obtained rotating the quantization axis in the two conductors independently by applying the transformation $S_{\theta_1,\theta_2}=\mathcal{U}S\mathcal{U}^\dagger$, where $\mathcal{U}$ is the rotation matrix given by

$$\mathcal{U}=\begin{pmatrix} \mathbb{I} & 0 & 0 \\ 0 & U_{\theta_1} & 0 \\ 0 & 0 & U_{\theta_2} \end{pmatrix} \tag{54}$$

and $U_\theta$ is defined in Eq. (26). This procedure is valid as long as no back scattering is present in the conductors. The probability distributions are given by Eqs. (18) and (19) where the state $|\psi\rangle$ is now factorizable:

$$|\psi\rangle=a^\dagger_{3\uparrow}(E)a^\dagger_{3\downarrow}(E)|0\rangle \tag{55}$$

in the energy range $0<E<eV$. Analogously to what was done in Sec. III A, when both analyzers are present we set $\sigma=\sigma'=\uparrow$. When only one analyzer is present, however, one has to use the correct characteristic function of Eq. (21), since one of the two additional correlators does not vanish. Namely, $\langle\hat{N}_{\mathrm{O}}^{1\uparrow}\hat{N}_{\mathrm{O}}^{1\downarrow}\rangle=\epsilon^2$ and $\langle\hat{N}_{\mathrm{O}}^{1\uparrow}\hat{N}_{\mathrm{O}}^{1\downarrow}\hat{N}_{\mathrm{O}}^{2\uparrow}\rangle=0$, when the upper analyzer, for example, in Fig. 8, is removed. For the other expectation values we get

$$\langle\psi|\hat{N}_{\mathrm{O}}^{1\uparrow}|\psi\rangle=\langle\psi|\hat{N}_{\mathrm{O}}^{2\uparrow}|\psi\rangle=\epsilon, \tag{56}$$

$$\langle\psi|\hat{N}_{\mathrm{O}}^{1\downarrow}|\psi\rangle=\epsilon, \tag{57}$$

$$\langle\psi|\hat{N}_{\mathrm{O}}^{1\uparrow}\hat{N}_{\mathrm{O}}^{2\uparrow}|\psi\rangle=\epsilon^2\sin^2\left(\frac{\theta_1-\theta_2}{2}\right), \tag{58}$$

and

$$\langle\psi|\hat{N}_{\mathrm{O}}^{1\downarrow}\hat{N}_{\mathrm{O}}^{2\uparrow}|\psi\rangle=\epsilon^2\cos^2\left(\frac{\theta_1-\theta_2}{2}\right), \tag{59}$$

obtaining the joint probability distributions reported in the Appendix. The above number operator expectation values are equal to the case of the entangler when $\epsilon$ is replaced by $T/2$, whereas the cross-terminal correlators are equal in the two cases if $\epsilon$ is replaced with $T/\sqrt{2}$. From this the follows that the characteristic functions for the beam splitter possess the same dependence on the angle difference as the corresponding characteristic functions for the entangler (Sec. III A) but have a different structure as far as scattering probabilities are concerned. In particular, as expected,[36] the cross-correlations vanish when the two angles are equal. On the contrary, when the angle difference is $\pi$ cross-correlations are maximized. Furthermore, when only one analyzer is present the characteristic function shows no dependence on the angle, but it is not factorizable, in contrast to the case of the entangler. As a result, the single terminal probabilities, given by Eq. (18), are equal in the two cases provided that $\epsilon$ is replaced with $T/2$. The joint probabilities for $Q_1=Q_2=M$ are equal in the two cases if $\epsilon$ is replaced with $T/\sqrt{2}$ (however, this replacement is not valid, in general, for joint probabilities with $Q_1,Q_2\neq M$):

$$P^{\theta_1,\theta_2}(M,M)=\left[\epsilon^2\sin^2\left(\frac{\theta_1-\theta_2}{2}\right)\right]^M, \tag{60}$$

$$P^{\theta_1,-}(M,M)=\epsilon^{2M}. \tag{61}$$

The no-enhancement assumption is verified when

$$\epsilon\leqslant\frac{1}{2}\,\frac{2^{Q/(M-Q)}-1}{2^{Q/(M-Q)}-\frac{1}{2}}, \tag{62}$$

which equals the condition of Eq. (34) once $\epsilon$ is replaced with $T/2$. Let us first consider the case for which $Q_1=Q_2=M$. We obtain an important result: the CH inequality is violated for the same set of angles found for the case of the entangler, although to a lesser extent, since the prefactors in Eqs. (60) and (61) now vary in the range $0\leqslant\epsilon^{2M}\leqslant 1/4^M$. In particular, in the simplest case of $M=1$, corresponding to injecting a single pair of electrons, the maximum violation corresponds to $\mathcal{S}_{CH}=(\sqrt{2}-1)/4$, which is half of the value for the entangler. Furthermore, the plot in Fig. 2 is also valid in the present case with $\overline{\mathcal{S}}_{CH}$ defined as $\overline{\mathcal{S}}_{CH}=\mathcal{S}_{CH}/\epsilon^{2M}$, i.e., by replacing $T/\sqrt{2}$ with $\epsilon$. This means that a geometry like that of the beam splitter enables to detect violation of CH inequality without any need to resort to interaction processes to produce entanglement.

Also here we consider the case for which $Q_1=Q_2\equiv Q<M$, where interesting differences with respect to the case of the entangler are found.

(i) We find that the violation of the CH inequality is in general weaker, meaning that the absolute maximum value of $\mathcal{S}_{CH}$ is smaller than in the ideal case of the entangler.

(ii) The weakening of the violation with increasing $M$ is determined by the suppression of the probability by the prefactor $(\epsilon^2)^{Q1+Q2}$. Remarkably, the maximum value of $\mathcal{S}_{\max}$ decreases like $1/M$, therefore even slower than for the ideal case.

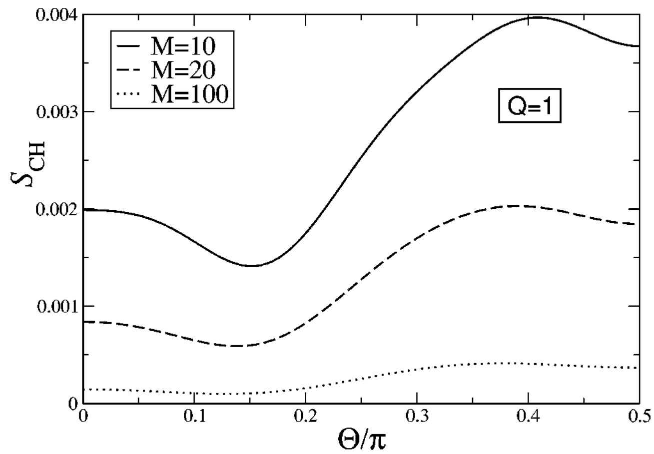


FIG. 9. The quantity $\mathcal{S}_{CH}$ for a normal beam splitter is plotted as a function of the angle $\Theta$ for three values of $M=eVt/h=10,20,100$ when $Q=1$. Interestingly, $\mathcal{S}_{CH}$ is positive for every angle and its maximum value decreases like $1/M$.

(iii) Violations occur only for values of $Q$ close to 1, even for large values of $M$: to search for violations one has to look at single- or few-pair probabilities and therefore, because of the no-enhancement assumption, to small transmissions $\epsilon$.

(iv) Interestingly, for $Q=1$ the quantity $\mathcal{S}_{CH}$ is positive for any angles, although the largest values correspond to $\Theta$ close to $\pi/2$ (see Fig. 9). We do not find any relevant variation, with respect to the discussion in paragraph Sec. III A, for probabilities relative to $Q_1 \neq Q_2$.

It is easy to convince oneself that, for an incident state composed of a single pair of particles impinging from the entering arm of the beam splitter (55), we obtain a final state $|\psi\rangle_{out}$ that contains an entangled part:

$$|\psi\rangle_{out}=\epsilon(b^{\dagger}_{1\uparrow}b^{\dagger}_{2\downarrow}-b^{\dagger}_{1\downarrow}b^{\dagger}_{2\uparrow})|0\rangle+\epsilon\, b^{\dagger}_{1\uparrow}b^{\dagger}_{1\downarrow}|0\rangle+\epsilon\, b^{\dagger}_{2\uparrow}b^{\dagger}_{2\downarrow}|0\rangle. \tag{63}$$

In Ref. 48 this fact was already noticed. For mesoscopic conductors, entanglement without interaction for electrons injected from a Fermi sea has been also discussed by Beenakker *et al.*[21] In the limit of strongly asymmetric beam splitter the state (63) is analogous to the one discussed in Ref. 21.

## IV. CONCLUSIONS

In mesoscopic multiterminal conductors it is possible to observe violations of locality in the whole distribution of the transmitted electrons. In this paper we have derived and discussed the CH inequality for the full counting electron statistics. In an idealized situation in which one supposes the existence of an *entangler*, we have found that the CH inequality is violated for joint probabilities relative to an equal number of electrons that have passed in different terminals. This is related to the intuition that any violation is lost in absence of coincidence measurements. The extent of the violation is suppressed for increasing $M$ (average number of injected pairs); however, such a suppression does not scale exponentially with $M$ like the probability, but instead decreases like $1/M^2$. This means that the detection of violation does not become exponentially difficult with increasing $M$. For fixed transport properties we analyzed the conditions, in terms of $M$ and number of counted electrons, for maximizing the violation of the CH inequality.

The violation of the CH inequality could be achieved in an experiment. Indeed we tested the CH inequality for two different realistic systems, namely, a normal beam splitter and a superconducting beam splitter. Interestingly we find a violation even for the normal system, even though weaker with respect to the idealized case of the entangler. In this case the violation is again suppressed for increasing observation time, but scales like $1/M$. We analyzed the superconducting case in the limit of small transmissivity and we also find a violation of the CH inequality to the same extent with respect to the case of the entangler.

It is important to notice that the analyzers should not affect the scattering properties of the system as in the case of ferromagnetic electrodes. In the latter case, in fact, the probability density of the local hidden variables would also depend on the angles $\theta_1$ and $\theta_2$.

We believe that the results derived in this work may be of interest for the understanding of the statistics of electrons in mesoscopic conductors. It is, however, important to look for experimental tests of our claims. In this respect two possible schemes for measuring the counting statistics have been recently proposed in Ref. 49. Since solid-state devices are considered promising implementations for quantum computational protocols, this line of research does not seem interesting only from a fundamental point of view, but may be of clear relevance for the actual realization of solid-state computers.

## ACKNOWLEDGMENTS

The authors would like to thank M. Büttiker, P. Samuelsson, and E. Sukhorukov for helpful discussions and C.W.J. Beenakker for comments on the manuscript. This work was supported by the EU (IST-FET-SQUBIT, RTN-Spintronics, RTN-Nanoscale Dynamics).

## APPENDIX: PROBABILITY DISTRIBUTIONS

In this appendix we give the general expressions for the joint probability distributions used in the paper to discuss the CH inequality.

### 1. Entangler

In the case of an entangler we find

$$P^{\theta_1,-}(Q_1,Q_2)=\frac{T^{(Q_1+Q_2)}}{2^M}\binom{M}{Q_1}\binom{M}{Q_2} \times(2-T)^{M-Q_1}(1-T)^{M-Q_2}, \tag{A1a}$$

$$P^{-,\theta_2}(Q_1,Q_2)=\frac{T^{(Q_1+Q_2)}}{2^M}\binom{M}{Q_1}\binom{M}{Q_2}\times(1-T)^{M-Q_1}(2-T)^{M-Q_2}, \quad \text{(A1b)}$$

and

$$P^{\theta_1,\theta_2}(Q_1,Q_2)=\sum_{k=\max[Q_1,Q_2]}^{\min[Q_1+Q_2,M]}\binom{M}{k}\binom{k}{2k-Q_1-Q_2}\times\binom{2k-Q_1-Q_2}{k-Q_2}\frac{T^{(Q_1+Q_2)}}{2^M}\times\left[2(1-T)+T^2\sin^2\left(\frac{\theta_1\pm\theta_2}{2}\right)\right]^{M-k}\times\left[1-T\sin^2\left(\frac{\theta_1\pm\theta_2}{2}\right)\right]^{2k-Q_1-Q_2}\times\left[\sin^2\left(\frac{\theta_1\pm\theta_2}{2}\right)\right]^{Q_1+Q_2-k}. \quad \text{(A2)}$$

### 2. Normal beam splitter

The joint probability $P^{\theta_1,\theta_2}(Q_1,Q_2)$ used in Sec. III C is

$$P^{\theta_1,\theta_2}(Q_1,Q_2)=\sum_{k=\max[M-Q_1,M-Q_2]}^{\min[(M-Q_1)+(M-Q_2),M]}\binom{M}{k}\binom{k}{M-Q_2}\times\binom{M-Q_2}{Q_1-M+k}\epsilon^{(Q_1+Q_2)}\left[1-2\epsilon+\epsilon^2\sin^2\left(\frac{\theta_1-\theta_2}{2}\right)\right]^{2M-Q_1-Q_2-k}\times\left[1-\epsilon\sin^2\left(\frac{\theta_1-\theta_2}{2}\right)\right]^{Q_1+Q_2-2M+2k}\times\left[\sin^2\left(\frac{\theta_1-\theta_2}{2}\right)\right]^{M-k}. \quad \text{(A3)}$$

The single-analyzer joint probability $P^{-,\theta_2}(Q_1,Q_2)$ reads

$$P^{-,\theta_2}(Q_1,Q_2)=\epsilon^{(Q_1+Q_2)}\sum_{k=0}^{Q_1}\sum_{l=\max[0,(Q_1-k)+(Q_2-k)]}^{\min[M-k,Q_2]}\binom{M}{k}\times\binom{M-k}{l}\binom{k}{k+l-Q_2}\binom{k+l-Q_2}{Q_1-k}\times[1-3\epsilon+2\epsilon^2]^{M-k-l}[1-\epsilon]^l\times[2-3\epsilon]^{2k+l-Q_1-Q_2} \quad \text{(A4)}$$

with $0\leqslant Q_1\leqslant 2M$ and $0\leqslant Q_2\leqslant M$ (note that the sum on $l$ has to be performed only when the lower limit is less than or equal to the upper limit).

### 3. Superconducting beam splitter

The joint probability $P^{\theta_1,\theta_2}(Q_1,Q_2)$ used in Sec. III B is

$$P^{\theta_1,\theta_2}(Q_1,Q_2)=\sum_{k=\max[Q_1,Q_2]}^{\min[Q_1+Q_2,M]}\binom{M}{k}\binom{k}{2k-Q_1-Q_2}\times\binom{2k-Q_1-Q_2}{k-Q_2}\left[\frac{A^8}{[A-T(A-1)]^8}\right]^M\times\left(\frac{2T^2}{A^2}\right)^k\left[1-4T+6T^2+\frac{2T^2}{A^2}\sin^2\left(\frac{\theta_1+\theta_2}{2}\right)\right]^{M-k}\times\left[\sin^2\left(\frac{\theta_1+\theta_2}{2}\right)\right]^{Q_1+Q_2-k}\times\left[\cos^2\left(\frac{\theta_1+\theta_2}{2}\right)\right]^{2k-Q_1-Q_2}, \quad \text{(A5)}$$

where $A=1+\tau_{hp}\tau_{hp}'^{*}$.

The single-analyzer joint probability $P^{-,\theta_2}(Q_1,Q_2)$ reads

$$P^{-,\theta_2}(Q_1,Q_2)=\binom{M}{Q_1}\binom{Q_1}{Q_2}\left(\frac{A^8}{[A-T(A-1)]^8}\right)^M\left(\frac{2T^2}{A^2}\right)^{Q_1}\times[1-4T+6T^2]^{M-Q_1} \quad \text{(A6)}$$

for $Q_1\geqslant Q_2$ and $P^{-,\theta_2}(Q_1,Q_2)=0$ for $Q_1<Q_2$.

[1] J.S. Bell, *Speakable and Unspeakable in Quantum Mechanics* (Cambridge University Press, Cambridge, England, 1987).
[2] M. Nielsen and I. Chuang, *Quantum Computation and Quantum Communication* (Cambridge University Press, Cambridge, England, 2000).
[3] A. Zeilinger, Rev. Mod. Phys. **71**, S288 (1999).
[4] A. Rauschenbeutel, G. Nogues, S. Osnaghi, P. Bertet, M. Brune, J.-M. Raimond, and S. Haroche, Science **288**, 2024 (2000).
[5] C.A. Sackett, D. Kielpinski, B.E. King, C. Langer, V. Meyer, C.J. Myatt, M. Rowe, Q.A. Turchette, W.M. Itano, D.J. Wineland, and C. Monroe, Nature (London) **404**, 256 (2000).
[6] D. Loss and D.P. DiVincenzo, Phys. Rev. A **57**, 120 (1998).
[7] Yu. Makhlin, G. Schön, and A. Shnirman, Rev. Mod. Phys. **73**, 357 (2001).
[8] *Semiconductor Spintronics and Quantum Computation*, edited by D.D. Awschalom, D. Loss, and N. Samarth, Series on Nanoscience and Technology (Springer-Verlag, Berlin, 2002).
[9] G. Burkard, D. Loss, and E.V. Sukhorukov, Phys. Rev. B **61**, R16303 (2000).
[10] F. Taddei and R. Fazio, Phys. Rev. B **65**, 075317 (2002).
[11] The idea behind these approaches is to use the superconductor as a source of singlet pairs (the Cooper pairs).
[12] D. Loss and E.V. Sukhorukov, Phys. Rev. Lett. **84**, 1035 (2000).

[13] P. Recher, E.V. Sukhorukov, and D. Loss, Phys. Rev. B **63**, 165314 (2001).
[14] G.B. Lesovik, T. Martin, and G. Blatter, Eur. Phys. J. B **24**, 287 (2001).
[15] P. Samuelsson, E.V. Sukhorukov, and M. Büttiker, Phys. Rev. Lett. **91**, 157002 (2003).
[16] P. Recher and D. Loss, Phys. Rev. B **65**, 165327 (2002).
[17] C. Bena, S. Vishveshwara, L. Balents, and M.P.A. Fisher, Phys. Rev. Lett. **89**, 037901 (2002).
[18] V. Bouchiat, N. Chtchelkatchev, D. Feinberg, G.B. Lesovik, T. Martin, and J. Torres, Nanotechnology **14**, 77 (2003).
[19] D.S. Saraga and D. Loss, Phys. Rev. Lett. **90**, 166803 (2003).
[20] A.T. Costa and S. Bose, Phys. Rev. Lett. **87**, 277901 (2001).
[21] C.W.J. Beenakker, C. Emary, M. Kindermann, and J.L. van Velsen, Phys. Rev. Lett. **91**, 147901 (2003).
[22] F. Plastina, R. Fazio, and M. Palma, Phys. Rev. B **64**, 113306 (2001).
[23] O. Buisson and F.W.J. Hekking, in *Macroscopic Quantum Coherence and Quantum Computing*, edited by D.V. Averin, B. Ruggiero, and P. Silvestrini (Kluwer, New York, 2001), p. 137.
[24] F. Marquardt and C. Bruder, Phys. Rev. B **63**, 054514 (2001).
[25] F. Plastina and G. Falci, Phys. Rev. B **67**, 224514 (2003).
[26] J.Q. You, J.S. Tsai, and F. Nori, Phys. Rev. Lett. **89**, 197902 (2002).
[27] J.S. Bell, Physics (Long Island City, N.Y.) **1**, 195 (1964).
[28] S. Kawabata, J. Phys. Soc. Jpn. **70**, 1210 (2001).
[29] N.M. Chtchelkatchev, G. Blatter, G.B. Lesovik, and T. Martin, Phys. Rev. B **66**, 161320 (2002).
[30] P. Samuelsson, E.V. Sukhorukov, and M. Büttiker, Phys. Rev. Lett. **92**, 026805 (2004).
[31] C.W.J. Beenakker and M. Kindermann, Phys. Rev. Lett. **92**, 056801 (2004).
[32] A central issue of these works is the ability to perform coincidence measurements which can be achieved by performing short-time measurement (Refs. 28 and 29), by operating in the tunneling limit (Refs. 15 and 21) or even for any transmission rates (Ref. 30).
[33] J.F. Clauser and M.A. Horne, Phys. Rev. D **10**, 526 (1974).
[34] L. Mandel and E. Wolf, *Optical Coherence and Quantum Optics*, (Cambridge University Press, Cambridge, England, 1995).
[35] The CH inequality given in Eq. (5) is said to be weak in the sense that it holds only when the no-enhancement assumption, Eq. (3), is satisfied.
[36] L.S. Levitov and G.B. Lesovik, Pis'ma Zh. Eksp. Teor. Fiz. **58**, 225 (1993) [JETP Lett. **58**, 230 (1993)].
[37] L.S. Levitov, H. Lee, and G.B. Lesovik, J. Math. Phys. **37**, 10 (1996).
[38] Yu.V. Nazarov, Ann. Phys. (Leipzig) **8**, Special Issue, SI-193 (1999).
[39] W. Belzig and Yu.V. Nazarov, Phys. Rev. Lett. **87**, 067006 (2001); **87**, 197006 (2001).
[40] L.S. Levitov, in *Quantum Noise in Mesoscopic Physics*, edited by Yu. V. Nazarov (Kluwer, Amsterdam, 2003); M. Kindermann and Yu. V. Nazarov, *ibid.*; D. A. Bagrets, and Yu. V. Nazarov, *ibid.*; W. Belzig, *ibid.*.
[41] M. Büttiker, Phys. Rev. B **46**, 12 485 (1992).
[42] B.A. Muzykantskii and D.E. Khmelnitskii, Phys. Rev. B **50**, 3982 (1994).
[43] A. Brataas, Yu.V. Nazarov, and G.E.W. Bauer, Eur. Phys. J. B **22**, 99 (2001).
[44] J. Börlin, W. Belzig, and C. Bruder, Phys. Rev. Lett. **88**, 197001 (2002).
[45] P. Samuelsson and M. Büttiker, Phys. Rev. Lett. **89**, 046601 (2002).
[46] S. Datta, *Electronic Transport in Mesoscopic Systems* (Cambridge University Press, Cambridge, England, 1995).
[47] M. Büttiker, Y. Imry, and M.Ya. Azbel, Phys. Rev. A **30**, 1982 (1984).
[48] S. Bose and D. Home, Phys. Rev. Lett. **88**, 050401 (2002).
[49] Yu.V. Nazarov and M. Kindermann, Eur. Phys. J. B **35**, 413 (2003).